Diffusion and Molecular Dynamics of Lipo-Fullerenes in Phospholipid Membranes Studied by NMR and Quasi-Elastic Neutron Scattering

Michael Hetzer,[†] Paul Karakatsanis,[†] Helene Casalta,[‡] Andreas Hirsch,[§] Xavier Camps,[§] Otto Vostrowsky,[§] and Thomas M. Bayerl*[,†]

Institut für Experimentelle Physik V, Universität Würzburg, D-97074 Würzburg, Germany, Institut Max von Laue-Paul Langevin, Avenue des Martyrs, 38042 Grenoble Cedex 9, France, and Institut für Organische Chemie, Universität Erlangen-Nürnberg, D-91054 Erlangen, Germany

Received: January 6, 2000; In Final Form: March 30, 2000

Lipo-fullerenes are lipophilic C_{60} derivatives (six pairs of alkyl chains symmetrically grafted to the C_{60} cage) that intercalate in phospholipid bilayers by the formation of rodlike structures of nanoscopic dimensions. Proton NMR measurements in the fringe field of a superconducting magnet (SFF-NMR) were employed to measure the long-range self-diffusion of lipo-fullerenes intercalated in oriented multilayers of dipalmitoylphosphatidylcholine (DPPC) between 27 and 70 °C. The lipo-fullerene diffusion was found to be an order of magnitude slower than that of the DPPC in the host bilayer. The lipo-fullerene diffusion continued largely unaffected even under conditions when the host bilayer assumed a solidlike gel state, indicating a decoupling of lipo-fullerene and DPPC motion. Quasi-elastic neutron scattering (QENS) was used to study the molecular dynamics of the lipo-fullerenes within the bilayer at four energy resolutions of the spectrometer (1, 19, 62, and 500 μeV), covering selectively the gighertz to terahertz frequency range of molecular motion. We find that the molecular dynamics in this frequency range is dominated by the motion of the 12 alkyl chains attached to each C_{60}. At 25 °C where both the DPPC and the lipo-fullerenes are in a solidlike state, the dynamics of the latter is dominated by kink defects of the alkyl chains at high frequency (terahertz range) and alkyl chain jumps at lower frequency gighertz range). At 75 °C where both components are fluid, the lipo-fullerene dynamics can be described by a superposition of segmental rotational motion of chains and a spatially restricted diffusion of the chain inside a spherical volume. The radii of the volumes were found to scale linearly with the distance of the chain segment from the fullerene cage.

Introduction

Lipo-fullerenes are lipophilic fullerene derivatives consisting of six pairs of alkyl chains (C_{12} or C_{18}) attached covalently to the C_{60} fullerene cage onto octahedral sites (T_h symmetry) denoted in the following by C_{60}−$HADC_{12}$ and C_{60}−$HADC_{18}$ respectively (Figure 1). C_{60}−$HADC_{18}$ as a bulk system exhibits an interesting phase behavior:[1] At 25 °C the C_{18} alkyl chains are in a predominantly all-trans state pointing away from the fullerene cage in a radial direction. This conformation results in a distorted cubic packing with an average distance between adjacent fullerene cages (separation distance) of approximately twice the alkyl chain length. Increasing the temperature of the bulk system to 75 °C causes the system to undergo two major structural transitions. The first is a partial intercalation (interdigitation) of the alkyl chains of adjacent lipo-fullerenes at 55 °C, resulting in an increase of the packing density by a decrease of the separation distance. The second transition at 64 °C is characterized by a complete melting of the chains, giving rise to a viscous fluid state with the lowest separation distance. In contrast, C_{60}−$HADC_{12}$ has alkyl chains with four fewer methylene groups and exhibits at all temperatures above 0° the viscous fluid state.

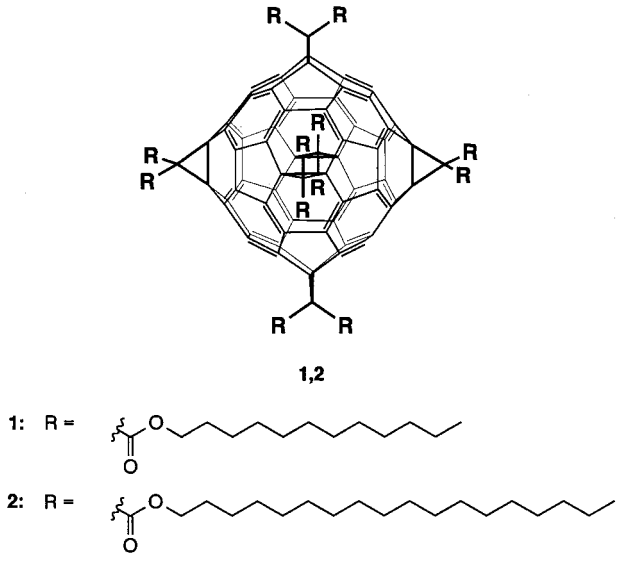

Figure 1. Structure of the lipo-fullerenes C_{60}−$HADC_{12}$ and C_{60}−$HADC_{18}$.

An intriguing property of the lipo-fullerenes is their ability to intercalate into phospholipid model membranes (bilayers) at high amounts without any significant disturbance of the bilayer phase behavior and molecular order.[2] The reason for this unusual behavior is the self-organized formation of a network of lipo-fullerene rods (rod diameter less than 30 nm) within the

* Corresponding author. Phone: ++49-931-888 5863. Fax: ++49-93-888 5851. E-mail: bayerl@physik.uni-wuerzburg.de.
[†] Universität Würzburg.
[‡] Institut Max von Laue-Paul Langevin.
[§] Universität Erlangen-Nürnberg.

10.1021/jp0000634 CCC: $19.00
Published on Web 05/19/2000

hydrophobic interior of the bilayer, which minimizes the contact area between the lipids and lipo-fullerenes. Nevertheless, the formation of this network has profound consequences for the bilayer micromechanic properties since it reinforces the bilayer structure and increases its bending modulus.[2] We have previously demonstrated that this composite system is the key for the creation of new materials such as nanoscopic hollow spheres with extraordinary physical properties.[3] However, the molecular mechanisms and forces that dominate the formation of these structures are at present largely unknown.

A deeper understanding of the self-organization of lipo-fullerenes in the bilayer and the formation of the composite structure requires knowledge of their diffusion properties and molecular dynamics. In this work we report a study of these physical properties by employing two powerful methods for the elucidation of dynamics: solid-state nuclear magnetic resonance (NMR) and quasi-elastic neutron scattering (QENS). By NMR we have studied the diffusion of the viscous-fluid lipo-fullerenes within a bilayer of a synthetic lecithin (DPPC) at temperatures that cover both the fluid and the gel state of the host membrane. QENS studies performed at different energy resolutions have allowed us to probe the molecular dynamics of the lipo-fullernes in the bilayer under conditions where the former were either in the viscous-fluid state (i.e., high packing density) or in the predominantly all-trans conformation (low packing density). The combination of the two methods allowed us to cover selectively a wide range of molecular correlation rates spanning from megahertz to terahertz frequencies, thus giving a rather comprehensive description of the dynamical processes in lipo-fullerene rods confined in lipid bilayers.

Materials and Methods

Materials and Sample Preparation. For both the SFF-NMR and QENS measurements, fully deuterated 1,2-dipalmitoyl-d_{31}-glycero-3-phosphocholine-d_{13} (DPPC-d_{75}) was used, which was purchased form Avanti Polar Lipids, Alabaster, AL. The lipo-fullerenes C_{60}−$HADC_{12}$ and C_{60}−$HADC_{18}$ (Figure 1) were synthesized as described in refs 2 and 4. Highly purified D_2O was purchased from Deuchem (Leipzig, Germany).

For NMR measurements oriented DPPC-d_{75} bilayers on glass substrates containing 20 mol % C_{60}−$HADC_{12}$ were prepared as described in ref 5. About 70 stacked glass plates (each 60 μm thick) were used as solid substrates for 30 mg of the lipo-fullerene/lipid mixture.

For the QENS measurements oriented DPPC-d_{75} bilayers containing 20 mol % C_{60}−$HADC_{18}$ were prepared as described in ref 6. Five highly polished, undoped silica wafers of 150 μm thickness and 5.0 cm diameter were used as solid substrates for 230 mg of the lipo-fullerene/lipid mixture.

Both NMR and QENS samples were fully hydrated (D_2O content 12 mol %) via the vapor phase. The water content of the samples was assessed by determining their phase transition temperatures T_m using differential scanning calorimetry (note that the lipo-fullerenes do not alter the T_m of DPPC-d_{75}[2]). By comparison with a T_m vs hydration calibration curve, the water content was determined with a precision of ±1 mol %.

NMR Self-Diffusion (SFF-NMR). Supercon Fringe Field (SFF) ^{1}H NMR diffusion measurements[7] were performed as described in detail in ref 5 using a stimulated echo pulse sequence ($90°_y-\tau_1-90°_y-\tau_2-90°_y-\tau_1-$(echo)) and a multiple excitation scheme.[7,8] The stimulated echo sequence allowed diffusion encoding during the τ_2 interval while the magnetization is stored along the z-axis and relaxation is solely determined by T_1 processes. First, τ_1 was kept fixed and an array of τ_2's was chosen. Fitting the resulting decay of the echo amplitudes with a single exponential gave the decay constant $s(\tau_1)$. The procedure was repeated for different τ_1 values. Finally, $s(\tau_1)$ was plotted against τ_1^2 and the resulting slope of this plot was $\gamma^2G^2D_0$ where γ is the gyromagnetic ratio, G is the fringe field gradient and D_0 is the diffusion constant. The τ_1 values were in the range of 20−120 μs. Appropriate τ_2 values were chosen to give a reasonable echo decay, and 500 transients were acquired for each echo amplitude with a repetition time of 2 s. The NMR spectrometer used was a 400 MHz Varian VXR type, and the magnetic field gradient at the sample position was $G = 58$ T/m ± 2%. Because of the finite bandwidth of the rf pulse (90° pulse length 2.5 μs) and the strong magnetic field gradient, only a thin slice of about 100 μm thickness of the oriented sample contributed to the signal. The error of sample temperature was less than 1 °C.

For the calculation of the diffusion constants D_0 we assumed a one-dimensional diffusion of the lipo-fullerenes within the bilayer plane. This seems justified because the lipo-fullerene rods extend over several micrometers along the bilayer plane but are less than 30 nm wide. The latter dimension is very small compared to the characteristic length scale of the SFF-NMR experiment which is $1/(\gamma G\tau_1)$ and thus is in the range of 1 μm. For the case of one-dimensional diffusion within the plane of the membrane with an angle θ between the direction of the diffusion (rod axis) and the field gradient vector the effective diffusion constant becomes $D_{eff} = D_0 \cos^2\theta$ where D_0 is the diffusion constant. For a random orientational distribution of rods in the bilayer plane one has to integrate over all angles θ and the stimulated echo amplitude is

$$A_{stim} = \frac{1}{2\pi}\int_0^{2\pi} \exp\left\{-\gamma^2G^2D_0(\cos^2\theta)\tau_1^2\left(\frac{2}{3}\tau_1 + \tau_2\right)\right\} d\theta$$

All other SFF-NMR data analysis was performed as described previously.[5]

Quasi-Elastic Neutron Scattering (QENS). Quasi-elastic scattering of C_{60}−$HADC_{18}$ intercalated in oriented stacks of nearly fully deuterated DPPC-d_{75} bilayers on silicon wafer substrates was measured by using the IN16 backscattering and the IN5 time-of-flight spectrometers at the Institute Max von Laue-Paul Langevin (Grenoble, France). The IN5 was used at incident wavelengths of 3, 6, and 9 Å, giving an energy resolution of 500, 62, and 19 μeV, respectively. The backscattering spectrometer IN16 had an incident wavelength of 6.271 Å corresponding to an energy resolution of 1 μeV (energy analysis by unpolished Si(111) crystals). The QENS experiments probed selectively a total time range of 10^{-12} to 10^{-9}s. The orientation of the sample in the neutron beam was such that the momentum transfer q was directed essentially along the bilayer plane (135° angle between the sample normal and the incoming neutron beam). This allowed the observation of molecular motion of the lipo-fullerenes along this plane while the contribution of the lipids was negligible due to the use of nearly fully deuterated DPPC-d_{75} featuring a very low incoherent scattering. The remaining incoherent scattering of the lipids along with their coherent scattering was removed from the data by subtracting the spectrum of a pure DPPC-d_{75} sample (same hydration as above) obtained at the same temperature and orientation (background subtraction). QENS data were acquired at two temperatures (25 and 75 °C with an error of ±1 °C).

In the first step of QENS data analysis, an elastic line plus one Lorentzian line—convoluted with the resolution function of the spectrometer—were fitted to the incoherent scattering function $S_{inc}(q,\omega)$ for each momentum transfer value q sepa-

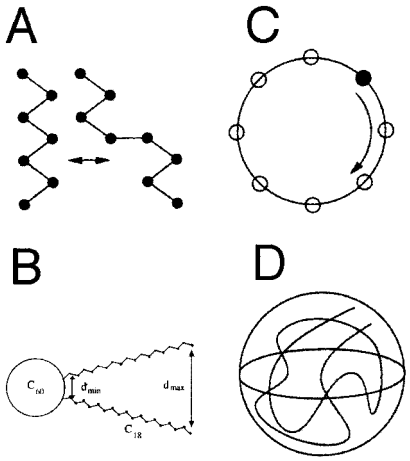

Figure 2. Schematic depiction of the four motional models used in the model dependent data analysis of QENS data. (A) Stochastic kinks jumping in alkyl chains.[9] (B) Jump diffusion between two equivalent sites.[10] (C) Segmental rotational diffusion.[11] (D) Chain translational diffusion inside a spherical volume.[12]

rately. This essentially model independent treatment of the data gave the elastic contribution to the spectrum in terms of the elastic incoherent structure factor (EISF) and the width (HWHM) Γ_1 of the Lorentzian line representing all motional contributions of the lipo-fullerenes resolvable at the given energy resolution. This single spectrum fitting procedure and the model dependent fitting procedure discussed below have been described in more detail previously.[6]

In a second step, a model dependent data analysis was performed. To select suitable models, it has to be appreciated that the incoherent scattering of the lipo-fullerenes is dominated by the vast amount of its alkyl chain protons. Further reasoning for the motional models considered are given in the Results and Discussion. The following models were considered; the equations of their scattering laws along with the incoherent structure factors as used in the model dependent fitting procedures are given in Appendix A.

(1) Stochastic kinks jumping in alkyl chains:[9] The stochastic appearance and disappearance of chain defects (kinks) at random sites along the chain (sketched in Figure 2A) is determined from the transition rates between the all-trans to the kink conformation (r_2) and back to the initial state (r_1). It follows that $r_1/(r_1 + r_2)$ is the probability for one kink per chain and $r_2/(r_1 + r_2)$ is the probability for the all-trans configuration. This model considers two Lorentzian lines of widths Γ_1 and Γ_2.

(2) Jump diffusion:[10] This model represents jumps of the chain protons between two equivalent sites separated by a distance d with a jump rate τ_r. We assumed a collective motion of the chain segment, resulting in a vibrational motion of the entire chain jumping over a distance d_{min} at one end and over d_{max} at the other end with a linear distribution between (Figure 2B). For $r_d = d_{min}/d_{max} = 0$ the bond between the fullerene cage and the chain prevents translational motion while for $r_d = 1$ the jump motion becomes isotropic. This model considers one elastic and one Lorentzian line.

(3) Segmental rotational diffusion:[11] The rotation of chain segments or of the entire alkyl chain (crank shaft motion) is equivalent to a continuous rotation of the protons on a circle (Figure 2C). Since there is no analytical expression for this model in a powder average, we approximated the continuous motion by rotational jump diffusion with N equivalent sites separated by a length l at a rate τ on a circle (radius r) where N is sufficiently large ($N = 16$). The fitting parameters were r and the jump rate τ.

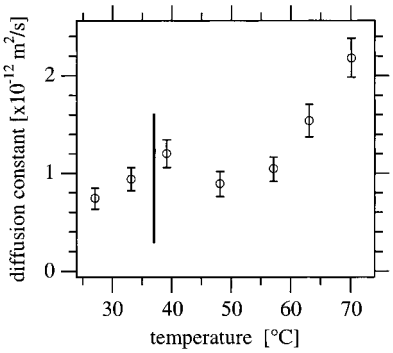

Figure 3. In-plane diffusion constant D_0 of C_{60}−$HADC_{12}$ in oriented DPPC-d_{62} multilayers at full hydration (12 mol % D_2O) vs temperature as measured by the SFF-NMR method. The vertical bar indicates the melting transition temperature of the DPPC host matrix.

(4) Chain translational diffusion inside a restricted (spherical) volume:[12] The volume accessible to a methylene group in an alkyl chain is assumed to be isotropic. The translational freedom of a segment of an alkyl chain bonded at one end to the fullerene cage depends on its position along the chain (Figure 2D). We assumed that the radii of the resulting diffusion spheres, r_V, were distributed linearly along the chain between a minimum $r_{V,min}$ (bound end) and a maximum radius $r_{V,max}$ (loose end). The parameter $r_r = r_{V,min}/r_{V,max}$ is defined analogously to that in model 2. The fitting procedure considered only one Lorentzian broadening. Its width Γ_1 can be approximated by $\Gamma_1 = 4.33D_V/r_V^2$ for small qr_V values and $\Gamma_1 = D_V q^2$ for large qr_V values (unrestricted diffusion).

For a superposition of independent motions, the resulting scattering function is the convolution of the corresponding dynamic structure factors for each motion.

Standard ILL procedures were applied for background and cell correction as well as normalization of the incoherent scattering to a vanadium standard sample.[6]

Results and Discussion

Measurement of Intermolecular Motions by NMR: Lateral Diffusion. Lateral diffusion of 20 mol % C_{60}−$HADC_{12}$ in a stack of oriented DPPC-d_{75} bilayers along the bilayer plane oriented perpendicular to the main magnetic field was measured as a function of temperature between 27 and 70 °C, thus covering the fluid and the gel state of the lipid host matrix. It should be noted that the alkyl chains of C_{60}−$HADC_{12}$ are in the fluid state over the whole temperature range studied according to microcalorimetry (DSC) results.[2]

Figure 3 shows a plot of the diffusion coefficient D_0 of the lipo fullerene C_{60}−$HADC_{12}$ along the membrane plane as a function of temperature. The values of D_0 are roughly 1 order of magnitude smaller than those obtained for the DPPC under fluid phase conditions by the same technique ($D_L = 2.3 \times 10^{-11}$ m^2/s ± 3% at 57 °C).[5]

Besides this slower diffusion compared to the lipid, the most striking feature is the persistence of C_{60}−$HADC_{12}$ lateral diffusion even under gel phase conditions of the host DPPC bilayer, i.e., at temperatures below 37 °C (indicated by a vertical bar in Figure 2). This is in marked contrast to the behavior of the DPPC, where lateral diffusion becomes about 4 orders of magnitude slower at the transition to the gel phase[13] and is rendered undetectable for SFF-NMR. Furthermore, there is a remarkably wide "plateau region" of D_0, extending from the DPPC phase transition temperature over 15 °C toward higher temperatures.

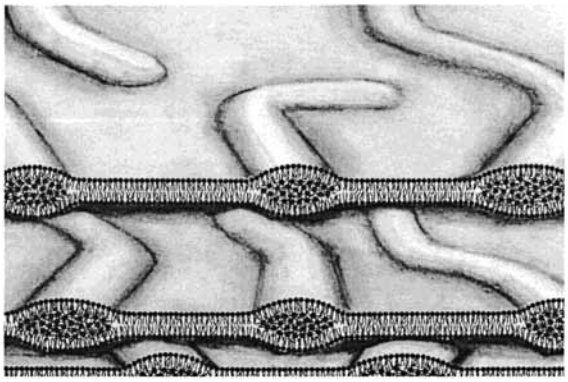

Figure 4. Schematic depiction of the arrangement lipo-fullerene rods within the hydrophobic interior of the lipid bilayer according to Hetzer.[2]

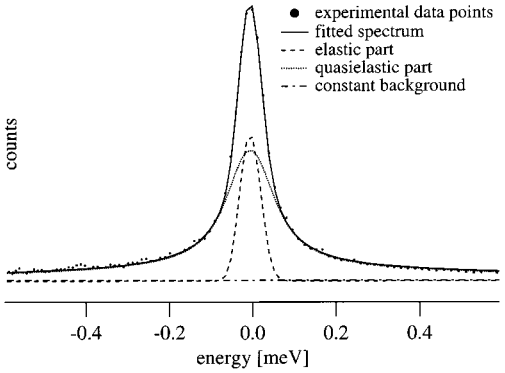

Figure 5. Example of the model independent data fitting of the QENS data (DPPC-d_{75} with 15 mol % C_{60}−$HADC_{18}$ at 75 °C, $q = 0.5$ Å^{-1}) by an elastic line plus one quasi-elastic (Lorentzian) line.

The free volume model of diffusion in a bilayer[14,15] predicts for molecules of comparable size and shape a constant value of $DM_w^{1/2}$, where D is the lateral diffusion constant and M_w is the molecular weight. This was experimentally confirmed for pyrenes and for pyrene derivatives.[14]

Considering $M_w = 3353$ for the lipo-fullerenes and $M_w = 734$ for DPPC this model would predict a value of D_0 for lipo-fullerene diffusion that is a factor of 2 slower than for the lipids. Hence, our results indicate that the free volume model is not applicable to the lipo-fullerene diffusion in bilayers.

On the contrary, our data suggest essentially a decoupling between the lipid and lipo-fullerene diffusion, most likely due to a spatial separation of the two components within the bilayer over distances above the experimental length scale of the SFF method (1−10 μm). This finding is in agreement with the structural model suggested previously for the DPPC/lipo-fullerene composite structure, where the existence of rodlike lipo-fullerene structures with rod lengths on the micrometer scale immersed within the bilayer was demonstrated by electron microscopy.[2] A schematic view of this arrangement is shown in Figure 4. In terms of this structural model, the diffusion within the up to 30 nm wide rods[2] is unaffected by the phase transition of the surrounding DPPC, except for those molecules situated directly at the interface (i.e., at the rod walls), because the C_{12} alkyl chains of the lipo-fullerenes remain fluid at all temperatures above 10 °C.

The previously reported change of the average length of the rods from several micrometers to less than 1 μm at the transition from the gel to the fluid state of the bilayer[2] may also explain the existence of the above-mentioned plateau region in Figure 2. This is because the shrinkage of the lipo-fullerene rod length below the length scale of the experiment at the phase transition of the lipids renders apparently unrestricted diffusion within the rod into a more restricted one. As a consequence, D_0 remains apparently constant with increasing temperature, as long as a decrease in mean free path length (i.e., rod length) is compensated by an increase in jump rate. Since our data show a further increase of D_0 of the lipo-fullerenes above 55 °C, this might indicate that the rods stopped shrinking above this temperature or that the diffusion of the short rod fragments as a whole within the bilayer become sufficiently large to contribute to the SFF experiment. In the latter case, the observed exponential increase of D_0 above 55 °C would be the result of a superposition of individual lipo-fullerene diffusion along the rod axis with the diffusion of whole short rod fragments (average length below 0.5 μm) within the fluid bilayer.

Measurement of Intramolecular Motions: QENS. Molecular motions of the lipo-fullerenes C_{60}−$HADC_{18}$ in a stack of oriented DPPC-d_{75} lipid bilayers were measured by QENS for two different temperatures corresponding to a crystal-like gel state of the sample (25 °C) and to a fluid state of both components (75 °C). C_{60}−$HADC_{18}$ rather than C_{60}−$HADC_{12}$ from the NMR was used in the QENS experiments because we were interested in the lipo-fullerene molecular dynamics under conditions of both fluid and rigid alkyl chains ($T_m = 64$ °C for C_{60}−$HADC_{18}$) while the C_{60}−$HADC_{12}$ is always fluid at temperatures above zero. Since both lipo-fullerenes behaved very similarly under fluid conditions from the NMR point of view,[2] this substitution should not limit significantly the comparison between the SFF and QENS data.

The length scale of the QENS experiments is estimated by $l = \pi/q_{min} \approx 1.5$ nm (q_{min} is the smallest momentum transfer with a quasielastic contribution to the spectrum). Since this is smaller than the radius of a single lipo-fullerene (2.8−6.1 nm, depending on the alkyl chain conformation[1]), only intramolecular (chain and segment dynamics) rather than intermolecular motions (translation or rotation of the entire molecule) can be observed by QENS. Within this context the observation of an anisotropy of lipo-fullerene dynamics imposed by the surrounding bilayer is not expected because of the dimension of the lipo-fullerene rods (30 nm in diameter). Therefore, all the motional models being tested were averaged to yield a powder distribution of directions.

Model Independent Analysis. This analysis was performed by fitting the QENS data by an elastic plus one quasi-elastic (Lorentzian) line. A typical example is shown in Figure 5. The results can be described by the elastic incoherent structure factor (EISF), which gives information on the geometry of the motion, and by the line width Γ_1 (HWHM) of the Lorentzian, which is determined by the correlation times of molecular motions in the resolved energy range. For all energy resolutions studied between 1 and 500 μeV the elastic incoherent structure factor (EISF) decreases with increasing momentum transfer q at 75 °C significantly faster than at 25 °C. For example, at a resolution of 62 μeV (IN5) and at $q = 1.5$ Å^{-1}, the EISF is 0.2 for 75 °C while it is 0.75 for 25 °C. This indicates a larger spatial extension of intramolecular motions at 75 °C. A simple q-axis scaling of the EISF values at 25 °C does not help to obtain an EISF decay similar to the one at 75 °C. This suggests some fundamental differences in the molecular dynamics of the lipo-fullerenes at the two temepratures since virtually all motional models of alkyl chains known from the literature exhibit an EISF scaling behavior as ql, where l is a characteristic length.

For all experiments the quasi-elastic part of the scattering function reveals a broader line width Γ_1 at 75 °C than at 25 °C, indicating a significantly faster motion at high temperatures. A plot of Γ_1 vs q^2 does not give a linear dependence for any of

TABLE 1: Fitting Results for the Segmental Jump−Chain Jump Model for 15 mol % C_{60}-$HADC_{18}$ in Oriented Multilayers of DPPC-d_{75} at 25 °C at Energy Resolutions of 500, 62, and 19 μeV (IN5) and of 1 μeV (IN16)

resolution	500 μeV	62 μeV	19 μeV	1 μeV
$r_d = d_{min}/d_{max}$	1	1	0	0
d_{max}/Å	1.1 ± 0.2	1.47 ± 0.06	8.6 ± 1.5	4.4 ± 0.14
jump rate $1/\tau_r$	320 ± 12 GHz	58 ± 5 GHz	170 ± 14 MHz	120 ± 5 MHz
kink per chain	0.85	0.78 ± 0.01	0.77 ± 0.02	
transition rate r_2		2.9 ± 0.3 GHz	3.7 ± 0.7 GHz	

the energy resolutions studied. Such a straight line having a zero ordinate intercept would be indicative of long-range diffusive motion. However, even at 1 μeV resolution and at 75 °C, where unrestricted diffusion is a likely contribution, no such dependence was observed. The diffusion of whole molecules as observed by SFF-NMR is still 1 order of magnitude too slow to contribute to QENS at the highest energy resolution (1 μeV). At this resolution we observed for both temperatures a Γ_1 that was largely independent of the momentum transfer, typical for spatially restricted motions.

Thus, for both temperatures the model independent analysis suggests the existence of two fundamentally different, but in both cases spatially restricted, types of molecular motion of the lipo-fullerenes in DPPC bilayers, with frequencies in the gigahertz to terahertz range.

Model Dependent Analysis. In a second step the QENS data were fitted to the four different motional models described in the Materials and Methods. None of these models alone provided acceptable fits to the data. Therefore, we attempted a combination of two models obtained by convoluting their individual scattering functions to fit the data. This implied the assumption that the single motions in the combined models were independent. For each temperature (25 and 75 °C) we found a different combination of two models to fit the data very well, in agreement with the model independent analysis that suggested two fundamentally different types of motion.

For 25 °C, a superposition of the stochastic-kink (model 1) and the chain jump-diffusion (model 2) motion (denoted the "kink jump−chain jump model" in the following) was the only two-model combination that provided good fits of the data. The validity of this model is further supported by an independent NMR and X-ray study of bulk lipo-fullerenes at different temperatures, which suggests an all-trans state of the chains at 20 °C.[1] Moreover, the existence of stochastic jumping of kinks in lipid chains of bilayers under gel phase conditions was demonstrated previously.[9]

For 75 °C, we obtained the best data fits for a combination of the segmental rotational diffusion (model 3) and chain diffusion-inside-a-sphere (model 4) which is denoted the "segment diffusion−chain diffusion model" in the following. Previous studies have provided ample evidence that the alkyl chains of C_{60}−$HADC_{18}$ are in a highly disordered ("molten") state at 75 °C. The two individual motional models used in this combination account for the dominating molecular motions under highly disordered conditions. In contrast, the "kink jump−chain jump model" used for fitting the data at 25 °C provided no acceptable fits of the 75 °C data.

Dynamics of Solidlike Chains (25 °C). The starting values for the fitting parameters of the "kink jump−chain jump model" model were taken from the best fitting results of the separately applied stochastic-kink and the two-site chain jump models. In a first step $r_d = d_{min}/d_{max} = 0.21$ (this ratio corresponds to the diameter of the fullerene cage over the total diameter of the all-trans lipo-fullerene molecule) was kept fixed, thus simulating an isotropic vibration around the center of mass of the lipo-fullerene molecule. The fitting procedure converged for all free parameters: the maximum jump distance, the jump rate, and the transition rates. In a second step, the parameter r_d was additionally set variable in order to explore the anisotropy of the vibration. For the high energy resolutions (1 and 19 μeV) the parameter r_d converged toward 0, as typical for a chain motion that is fixed at one end and free at the other. In contrast, for the lower energy resolutions (i.e., for high frequencies) r_d approached unity, indicative for isotropic motion. The fitting results are summarized in Table 1.

The jump rate at high energy resolution of less than 0.2 GHz and chain jump amplitudes d_{max} of 4−8 Å suggests, taking into account that $r_d = 0$, a jump motion of the chain inside a cone with an apex angle of 10−20°, with the immobile end of the chain attached to the fullerene cage. At lower resolution (500 and 62 μeV) the model suggests an isotropic motion of the chain segments at low amplitude (>1.5 Å) and a frequency in the 50−320 GHz range, which is at the upper limit of the detectable time scale. The differences in the geometry of the motions at high and low resolution can be understood on the basis of the different time scales connected with these resolutions. At short time scales the (isotropic) kink motion is the dominating contribution at 25 °C. At the higher energy resolution (i.e., longer time scale) the spectrometer becomes increasingly insensitive to the kink motion contribution and the slower (anisotropic) jump motion dominates the QENS signal.

Amplitudes in the range of 1 Å and the upper gigahertz frequency range are rather typical for stochastic kink motion in the solid state, and the results obtained for 62 μeV are comparable to what was observed previously for solid polyethylene.[16] However, the transition rates are about 1 order of magnitude slower than those measured for lipid chains at this temperature[9] suggesting constraints for fast kink motion in the lipo-fullerene chains. A possible reason could be the looser chain packing in the latter system compared to the tight packing of lipid chains in a bilayer. This would correspond to a significantly weaker van der Waals interaction potential experienced by adjacent fullerene chains and result in lower kink transition rates.

The loose packing would also explain the relatively high number of kinks (one kink at three out of four chains) indicated by our model. There is a considerable free volume predominantly toward the free chain end that the methylene protons can access.

To sum up, the "kink jump−chain jump" model suggests at 25 °C an anisotropic jump motion of the whole chain in the megahertz range superimposed upon the isotropic motion of a significant number of kink defects at higher frequency (gigahertz range).

Dynamics of Fluid Chains (75 °C). To keep the number of free parameters in the "segment diffusion−chain diffusion model" model low, we estimated the radius r_H for the segmental rotational diffusion from geometrical considerations. Although the C−C bonds along the chain can rotate freely, the C−C−C bond angle must remain constant, suggesting a synchronized rotation over several methylene groups, similar to a rotating crank shaft. The radius of the protons involved in this crank shaft motion is readily calculated to $r_H = 1.41$ Å from the bond

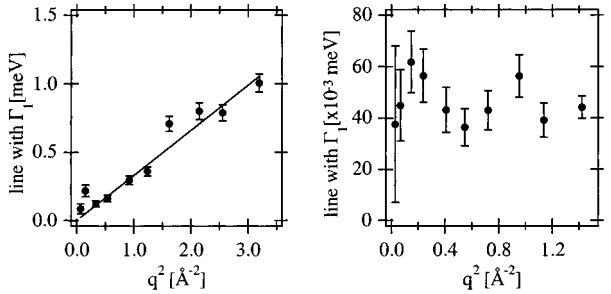

Figure 6. Line width Γ_1 of the quasi-elastic contribution of the volume diffusion part of the segment diffusion−chain diffusion model at 62 μeV (left) and 19 μeV (right) energy resolution and at a temperature of 75 °C.

TABLE 2: Fitting Results for the Segment Diffusion−Chain Diffusion Model for 15 mol % C_{60}−$HADC_{18}$ in Oriented Multilayers of DPPC-d_{75} at 75 °C at Energy Resolutions of 500, 62, and 19 μeV (IN5) and of 1 μeV (IN16)

resolution	500 μeV	62 μeV	19 μeV	1 μeV
volume diff const D_V (10^{-10} m^2 s^{-1})		8.9 ± 0.3	2.2 ± 0.6	1.7 ± 0.1
max. diameter sphere r_{max}		2.1 ± 0.1	3.9 ± 0.5	12.0 ± 0.3
rotational diff const D_r (10^9 s^{-1})	29 ± 1	14 ± 1	1.8 ± 0.2	

angles and C−C distances of an alkyl chain. In the first step of the fitting procedure this value was kept constant. The results are summarized in Table 2.

For $r_H = 1.41$ Å the fit gave rotational diffusion constants in a range 10^7 to 10^{10} s^{-1}, increasing with decreasing instrument resolution. This suggests a rotational motion extending over several orders of magnitude in frequency. Here each D_r value is representative of the sensitive time window at the corresponding resolution. Hence, the fitting model, which considers only two Lorentzian lines, fits for each experiment its "typical" frequency.

For the chain diffusion part of the model we started—similar to the chain jump model—with a value of 0.21 for the ratio $r_r = r_{min}/r_{max}$. When this parameter was allowed to vary in the fitting procedure, the procedure converged to zero for all resolutions. This suggests that the methyl protons close to the fullerene cage can access only a small volume for translational diffusion. This volume increases rather linearly with the distance from the "grafting point" of the alkyl chain. The maximum radius of the sphere accessible to the methylene protons r_{max} is different for each resolution and reflects the length scale of the experiment. This is not in contradiction to our earlier notion that diffusion beyond the limits of the experimental length scale is unrestricted and thus leads to a vanishing EISF. The convergence of r_r toward zero indicates that part of the scatterers close to the "grafting point" undergo restricted diffusion while those at the end of the chain can diffuse unrestricted in terms of the experimental length scale.

The q dependence of Γ_1 supports the above results. The theory of diffusion in a sphere predicts for a plot of Γ_1 vs q^2 a linear dependence in the limit $q^2r^2 > \pi$ and a q independence for $q^2r^2 < \pi$.[12] Figure 6 shows Γ_1 vs q^2 for different energy resolutions, as obtained from our data by fitting Γ_1 for each q value separately for a given resolution.

At 62 μeV resolution ($r_{max} = 2.1$ Å, cf. Table 2) we obtained a linear dependence with $\Gamma_1 \approx q^2$. This is because the length scale of this experiment is rather short (2.1 Å) and thus the spectrum is dominated by unrestricted diffusion. In contrast, at 19 μeV resolution (and at 1 μeV, not shown) we observe a Γ_1 that is q independent. Here we have a larger length scale (12 Å for 1 μeV) that is beyond the spatial variation of the methylenes, and thus restricted diffusion dominates the spectrum. Consequently, the volume diffusion constants D_V listed in Table 2 were obtained by fitting the 62 μeV data according to $\Gamma_1 = D_V q^2$, and to $\Gamma_1 = 4.33 D_V/r_{max}^2$ [12] for the 19 and 1 μeV resolutions, with D_V as the free parameter. Despite the wide range of time scales probed by the experiment, the obtained D_V values are all in the same order of magnitude (10^{-10} m^2/s, cf. Table 2).

In a final step of the fitting procedure the radius of the rotational diffusion r_H was set as a free parameter. For all experiments, r_H converged to values larger than the previously fixed 1.41 Å (about 2 Å for the 62 and 19 μeV resolutions). This may indicate that the true radius is somewhat larger than the one assumed on purely geometrical considerations.

Conclusions

The combination of QENS and NMR used in this work covers selectively a range of motional correlation times of more than 6 orders in magnitude. While the NMR technique detected exclusively the long-range diffusion, the QENS proved sensitive to the local motions of the alkyl chains grafted to the fullerene cage at a higher frequency. In particular, the QENS provided evidence for a drastic change in the molecular dynamics of the lipo-fullerenes, which is connected with the transition of the alkyl chains between a fluid and a more solidlike state. Since the NMR provided evidence for a complete spatial separation of the lipids and the lipo-fullerenes in the composite bilayer on a nanoscopic length scale, the question arises whether the lipid bilayer affects the molecular dynamics of the lipo-fullerenes at all if compared to a bulk system. Earlier studies suggest that the packing of the lipo-fullerenes in a bilayer is different from that in the bulk, possibly owing to the lower dimensionality of the lipo-fullerene rods. Specifically, partial interdigitation between the fullerene chains as observed in the bulk seems to be absent in the bilayer. The additional free volume due to this less efficient packing in the bilayer may cause a relatively large number of kinks at low temperature (25 °C) and may increase the spatial extension of segmental diffusion inside a sphere at 75 °C. Since the lipo-fullerene rods increase drastically the bending modulus of the bilayer,[2] it would be very interesting to correlate the molecular dynamics of the rod constituents with this macroscopic property. This will require comparative QENS experiments with the short-chain lipo-fullerene $HDAC_{12}$ (used in the NMR experiments), which are presently under way in our laboratory.

Acknowledgment. The expert help of Dr. Rainer Zorn (FZ Jülich) in the QENS data analysis is gratefully acknowledged. This work was supported by a grant from the Deutsche Forschungsgemeinschaft.

Appendix A

Summary of the scattering laws $S(Q,\omega)$ and their dynamic structure factors A_n considered in the model dependent data analysis. In the equations below, the following symbols were used: j_n = Bessel function of nth order, $\delta(\omega)$ = elastic signal, $L(\Gamma_n,\omega)$ = nth quasi-elastic contribution described by a Lorentzian.

(1) Stochastic Kink Diffusion.[9]

$$S(Q,\omega) = A_0(Q)\,\delta(\omega) + A_1(Q)\,L(\Gamma_1;\omega) + A_2(Q)\,L(\Gamma_2;\omega)$$

with structure factors

$$A_0(Q) = \frac{1}{(1+\rho)^2}\left[\rho^2 + \frac{13}{15}\rho + \frac{1417}{2160} + j_0(Qd_1)\left(\frac{2}{15}\rho + \frac{53}{720}\right) + j_0(Qd_2)\left(\frac{2}{15}\rho + \frac{251}{4320}\right) + j_0(Qd_3)\left(\frac{13}{15}\rho + \frac{917}{4320}\right)\right]$$

$$A_1(Q) = \frac{1}{1+\rho}\left[\frac{743}{2160} - \frac{53}{720}j_0(Qd_1) - \frac{251}{4320}j_0(Qd_2) - \frac{917}{4320}j_0(Qd_3)\right]$$

$$A_2(Q) = \frac{\rho}{(1+\rho)^2}\left[\frac{341}{432} - \frac{3}{720}j_0(Qd_1) - \frac{65}{864}j_0(Qd_2) - \frac{2827}{4320}j_0(Qd_3)\right]$$

and Lorentzian HWHM

$$\Gamma_1 = r_2 \qquad \text{and} \qquad \Gamma_1 = r_2 + 2r_1$$

Here d_n is the jump length due to the kink, $\rho/(1+\rho)$ is the probability for the all-trans configuration of the acyl chain and $r_{1,2}$ are the transition rates trans → gauche or gauche → trans, respectively.

(2) Jumping of Chain between Two Sites:[10]

$$S(Q,\omega) = \frac{1}{2}[1 + j_0(Qd)]\delta(\omega) + \frac{1}{2}[1 - j_0(Qd)]\frac{1}{\pi}\frac{2\tau}{4 + \omega^2\tau^2}$$

with τ^{-1} being the jump rate probability and d is the jump distance.

(3) Segmental Rotational Diffusion:[11]

$$S(Q,\omega) = A_0(Q)\delta(\omega) + \sum_{l=1}^{N-1} A_1(Q)\frac{1}{\pi}\frac{\tau_l}{1 + \omega^2{\tau_l}^2}$$

with structure factors

$$A_l(Q) = \frac{1}{N}\sum_{n=1}^{N} j_0(Qr_n)\cos\left(\frac{2nl\pi}{N}\right)$$

and

$$r_n = 2r\sin\left(\frac{n\pi}{N}\right) \qquad \frac{1}{\tau_1} = \frac{2}{\tau}\sin\left(\frac{l\pi}{N}\right)$$

In this model, τ_l is the correlation time for the l-th quasielastic line, r_n is the distance to site n and N represents the total number of sites.

(4) Chain Translational Diffusion Inside a Restricted (Spherical) Volume:[12]

$$S(Q,\omega) = A_0(Q)\,\delta(\omega) + \sum_{\{l,n\}\neq\{0,0\}} (2l+1)A_l^n(Q)\,L(\lambda_l^n D;\omega)$$

with structure factors

$$A_0^0(Q) = \left[\frac{3j_1(QR)}{QR}\right]^2$$

$$A_l^n(Q) = \frac{6R^2\lambda_l^n}{R^2\lambda_l^n - l(l+1)}\left[\frac{QRj_{l+1}(QR) - lj_l(QR)}{R^2[Q^2 - \lambda_l^n]}\right]^2 \qquad \text{for } Q^2 \neq \lambda_l^n$$

and

$$A_l^n(Q) = \frac{3}{2}j_l^2(R\sqrt{\lambda_l^n})\frac{R^2\lambda_l^n - l(l+1)}{R^2\lambda_l^n}$$

otherwise,

$$L(\lambda_l^n D;\omega) = \frac{1}{\pi}\frac{\lambda_l^n D}{(\lambda_l^n D)^2 + \omega^2}$$

the Lorentzian functions are given by In this model, λ_l is the eigenvalue of the l-th spherical harmonics function, R is the radius of the spherical boundary and D represents the diffusion constant.

References and Notes

(1) Hetzer, M.; Gutberlet, T.; Brown, M. F.; Camps, X.; Vostrowsky, O.; Schönberger, H.; Hirsch, A.; Bayerl, T. M. *J. Phys. Chem. A* **1999**, *103*, 637−642.

(2) Hetzer, M.; Bayerl, S.; Camps, X.; Vostrowsky, O.; Hirsch, A.; Bayerl, T. M. *Adv. Mater.* **1997**, *9*, 913−917.

(3) Hetzer, M.; Clausen-Schaumann, H.; Bayerl, S.; Bayerl, T. M.; Camps, X.; Vostrowsky, O.; Hirsch, A. *Angew. Chem., Int. Ed. Engl.* **1999**, *38*, 1962−1965.

(4) Camps, X.; Hirsch, A. *J. Chem. Soc. Perkin Trans.* **1997**, *1*, 1595−1596.

(5) Karakatsanis, P.; Bayerl, T. M. *Phys. Rev. E* **1996**, *54*, 1785−1790.

(6) König, S.; Pfeiffer, W.; Bayerl, T.; Richter, D.; Sackmann, E. *J. Phys. II* **1992**, *2*, 1589−1615.

(7) Kimmich, R.; Fischer, E. *J. Magn. Reson.* **1994**, *106*, 229−220.

(8) Fischer, E.; Kimmich, R.; Fatkullin, N. *J. Chem. Phys.* **1997**, *106*, 9883−9888.

(9) König, S.; Bayerl, T. M.; Coddens, G.; Richter, D.; Sackmann, E. *Biophys. J.* **1995**, *68*, 1871−1880.

(10) Bee, M. *Quasielastic Neutron Scattering. principles and Applications in Solid State Chemistry, Biology and Materials Science*; Adam Hilger: Bristol and Philadelphia, 1988.

(11) Dianoux, A. J.; Volino, F.; Hervet, H. *Mol. Phys.* **1975**, *30*, 1181−1194.

(12) Volino, F.; Dianoux, A. J. *Mol. Phys.* **1980**, *41*, 271−283.

(13) Wu, E. S.; Jacobson, K.; Papahadiopoulos, D. *Biochemistry* **1977**, *16*, 3936−3941.

(14) Galla, H.; Hartman, W.; Thielen, V.; Sackmann, E. *J. Membr. Biol.* **1979**, *48*, 215−236.

(15) Vaz, W. L. C.; Goodsaid-Zalduondo, F.; Jacobson, K. *FEBS Lett.* **1984**, *174*, 199−207.

(16) Bahar, I.; Erman, B. *J. Am. Chem. Soc.* **1986**, *20*, 1368−1376.